

Search for light gauge boson $Z_{\mu\tau}$ via $t\bar{t}h_1$ production at LHC

Jin-Xin Hou ^{*}, Chong-Xing Yue [†] and Yu-chen Guo [‡]

Department of Physics, Liaoning Normal University, Dalian 116029, China

Abstract

We consider the production of the new gauge boson $Z_{\mu\tau}$ predicted by the $U(1)_{L_\mu-L_\tau}$ model via SM-like Higgs boson h_1 decaying in the $t\bar{t}h_1$ production at LHC. Considering the current constraints on the relevant free parameters, we calculate its production cross section and further investigate the possibility of detecting $Z_{\mu\tau}$ through the process $pp \rightarrow t(\rightarrow bj\bar{j})\bar{t}(\rightarrow \bar{b}l^-\bar{\nu}_l)h_1(\rightarrow Z_{\mu\tau}Z_{\mu\tau}) \rightarrow b\bar{b}j\bar{j}l^-\bar{\nu}_l + \cancel{E}_T$ at LHC. We find that $Z_{\mu\tau}$ might be detected via this process at LHC with high integrated luminosity.

I. Introduction

The establishment of the particle physics Standard Model (SM) provides a good description of experiments over the wide range of energy scale from eV to TeV scale. Although the status of the SM has not been shaken for more than 30 years, it is not the end of the story! At present, there are several areas that new physics beyond SM may exist. The exploration of Dark Matter (DM), the observation of neutrino mass [1] and the discrepancy in the anomalous magnetic moment of muon ($g - 2$) [2, 3] from SM prediction are the most representative examples.

In order to resolve the muon ($g - 2$) anomalous magnetic moment's 3.6σ deviation from the SM prediction [4, 5], many extensions of the SM have been proposed so far. Among them, one of the minimal extensions is to add a new local $U(1)_{L_\mu-L_\tau}$ gauge symmetry to SM [6–8]. Therefore, the model's complete gauge group is $SU(3)_C \times SU(2)_L \times U(1)_Y \times U(1)_{L_\mu-L_\tau}$. Interestingly enough, the $U(1)_{L_\mu-L_\tau}$ gauge symmetry is an anomaly free extension, so it can also explain the neutrino mass and mixings simultaneously. In this model, the particle content of SM is extended by including three right-handed (RH) neutrinos and two SM gauge singlet scalars. The new particles are given appropriate $U(1)_{L_\mu-L_\tau}$ charge. One of the scalars picks up a Vacuum Expectation Value (VEV) breaking $U(1)_{L_\mu-L_\tau}$ symmetry spontaneously, while the other does not take any VEV. The new gauge boson $Z_{\mu\tau}$ after spontaneous breaking of $U(1)_{L_\mu-L_\tau}$ becomes massive and gives additional contribution to the muon ($g - 2$), helping reconcile the observed data with the theoretical prediction [9]. The recent researches have shown that the gauge boson mass and the gauge coupling constant should be of order 10 MeV and 10^{-4} respectively to explain the muon ($g - 2$) deviation. At the same time, they also proposed that the light and weakly interacting gauge boson can explain the deficit of cosmic neutrino flux reported by IceCube collaboration [10–13]. These important facts have made active searches of a new light gauge boson in various experiments. For example, meson decay

^{*}E-mail: houjinxin_email@yeah.net

[†]E-mail: cxyue@lnnu.edu.cn

[‡]E-mail: lgguo-yuchen@126.com

experiment [14], beam dump experiment [15], electron-positron collider experiment [16] and so on.

In this work, we will focus on the light gauge boson $Z_{\mu\tau}$ production from $t\bar{t}h$ associated production channel and the possibility to search for its signature at the LHC. We calculate $Z_{\mu\tau}$ production cross section by considering the current constraints on the relevant free parameters. Then, we investigate the observability of $Z_{\mu\tau}$ production through the $pp \rightarrow t(\rightarrow bj\bar{j})\bar{t}(\rightarrow \bar{b}l^-\bar{\nu}_l)h_1(\rightarrow Z_{\mu\tau}Z_{\mu\tau}) \rightarrow b\bar{b}j\bar{j}l^-\bar{\nu}_l + \cancel{E}_T$ channel. We analyze the signal significance depending on the integrated luminosity and find that this signal is promising at LHC with high integrated luminosity.

The paper is organized as follows. In Sec. II, we briefly review the element features of $U(1)_{L_\mu-L_\tau}$ model. The cross section of $Z_{\mu\tau}$ production at LHC is calculated in Sec. III. In Sec. IV, we investigate the signal observability and discovery potentiality of the $Z_{\mu\tau}$ production at LHC. Finally, we summarize our results in Sec. V.

II. The Element Features of $U(1)_{L_\mu-L_\tau}$ Model

The main purpose of proposing $U(1)_{L_\mu-L_\tau}$ extension of the SM is to explain the smallness of neutrino mass, explain the deviation of muon ($g-2$) and provide DM candidate. Recently, Ref. [9] has given a detailed study of the minimal gauge extension of SM, which is called $U(1)_{L_\mu-L_\tau}$ model. In the $U(1)_{L_\mu-L_\tau}$ model, where the L_μ and L_τ are the muon and tau lepton numbers respectively, the muon (μ) and tau (τ) flavor leptons are charged among the SM leptons. The complete gauge group of the model is $SU(3)_C \times SU(2)_L \times U(1)_Y \times U(1)_{L_\mu-L_\tau}$. The particle content of this model is given in Tables 1 and 2.

Table 1: Charges of all particles under SM gauge group.

Gauge Group	Baryon Fields			Lepton Fields			Lepton Fields		
	$Q_L^i = (u_L^i, d_L^i)^T$	u_R^i	d_R^i	$L_L^i = (v_L^i, e_L^i)^T$	e_R^i	N_R^i	ϕ_h	ϕ_H	ϕ_{DM}
$SU(2)_L$	2	1	1	2	1	1	2	1	1
$U(1)_Y$	1/6	2/3	-1/3	-1/2	-1	0	1/2	0	0

Table 2: Charges of all particles under $U(1)_{L_\mu-L_\tau}$ gauge group.

Gauge Group	Baryonic Fields	Lepton Fields			Lepton Fields		
	(Q_L^i, u_R^i, d_R^i)	(L_L^e, e_R, N_R^e)	$(L_L^\mu, \mu_R, N_R^\mu)$	$(L_L^\tau, \tau_R, N_R^\tau)$	ϕ_h	ϕ_H	ϕ_{DM}
$U(1)_{L_\mu-L_\tau}$	0	0	1	-1	0	1	$n_{\mu\tau}$

The Lagrangian of the model is given by [9]

$$\mathcal{L} = \mathcal{L}_{SM} + \mathcal{L}_N + \mathcal{L}_{DM} + (D_\mu \phi_H)^\dagger (D^\mu \phi_H) - V(\phi_h, \phi_H) - \frac{1}{4} F_{\mu\tau}^{\alpha\beta} F_{\mu\tau\alpha\beta}, \quad (1)$$

where \mathcal{L}_{SM} represents the Lagrangian of SM. The \mathcal{L}_N is the RH neutrinos Lagrangian. Since the RH neutrinos does not participate in operations, we do not give its specific form here. In Eq. (1), \mathcal{L}_{DM} is the dark matter Lagrangian which contains the kinetic term of the dark

matter candidate ϕ_{DM} and the interaction terms of ϕ_{DM} with the SM-like Higgs (ϕ_H). The expression of the \mathcal{L}_{DM} is as follows

$$\begin{aligned}\mathcal{L}_{DM} &= (D^\mu\phi_{DM})^\dagger(D_\mu\phi_{DM}) - \mu_{DM}^2\phi_{DM}^\dagger\phi_{DM} - \lambda_{DM}(\phi_{DM}^\dagger\phi_{DM})^2 \\ &\quad - \lambda_{Dh}(\phi_{DM}^\dagger\phi_{DM})(\phi_h^\dagger\phi_h) - \lambda_{DH}(\phi_{DM}^\dagger\phi_{DM})(\phi_H^\dagger\phi_H),\end{aligned}\quad (2)$$

where the λ_{DM} , λ_{Dh} and λ_{DH} are quartic couplings of the scalar fields. The fourth term in Eq. (1) represents the kinetic term of the extra Higgs singlet ϕ_H . The potential $V(\phi_h, \phi_H)$ contains the quadratic and quartic interactions of ϕ_H and the interaction term between ϕ_h and ϕ_H . The expression of the potential $V(\phi_h, \phi_H)$ is as follows

$$V(\phi_h, \phi_H) = \mu_H^2\phi_H^\dagger\phi_H + \lambda_H(\phi_H^\dagger\phi_H)^2 + \lambda_{hH}(\phi_h^\dagger\phi_h)(\phi_H^\dagger\phi_H).\quad (3)$$

The last term in the Eq. (1) is the kinetic energy term of the extra gauge boson $Z_{\mu\tau}$, in which the field strength tensor $F_{\mu\tau}^{\alpha\beta} = \partial^\alpha Z_{\mu\tau}^\beta - \partial^\beta Z_{\mu\tau}^\alpha$. The generic form of the covariant derivative contained in Eq. (1) is

$$D_\nu X = (\partial_\nu + ig_{\mu\tau}Q_{\mu\tau}(X)Z_{\mu\nu})X,\quad (4)$$

where X is any SM singlet field which has $U(1)_{L_\mu-L_\tau}$ charge $Q_{\mu\tau}(X)$ and $g_{\mu\tau}$ is the gauge coupling of the $U(1)_{L_\mu-L_\tau}$ gauge group. The $U(1)_{L_\mu-L_\tau}$ symmetry breaks spontaneously once ϕ_H picks up a VEV and consequently the extra gauge field becomes massive with mass term $M_{Z_{\mu\tau}} = g_{\mu\tau}v_{\mu\tau}$.

$$\phi_h = \begin{pmatrix} 0 \\ \frac{v+H}{\sqrt{2}} \end{pmatrix}, \quad \phi_H = \begin{pmatrix} \frac{v_{\mu\tau}+H_{\mu\tau}}{\sqrt{2}} \end{pmatrix},\quad (5)$$

where v and $v_{\mu\tau}$ are the VEVs of ϕ_h and ϕ_H respectively. The presence of the mutual interaction between ϕ_H and ϕ_h in Eq. (3) induces the mixing between H and $H_{\mu\tau}$. Hence, the scalar mixing matrix has the following form

$$\mathcal{M}_{scalar}^2 = \begin{pmatrix} 2\lambda_h v^2 & \lambda_{hH}v_{\mu\tau}v \\ \lambda_{hH}v_{\mu\tau}v & 2\lambda_H v_{\mu\tau}^2 \end{pmatrix}.\quad (6)$$

We see from the expression of \mathcal{M}_{scalar}^2 that if we take $\lambda_{hH} = 0$, then H and $H_{\mu\tau}$ can represent the physical states (zero mixing between H and $H_{\mu\tau}$). But in our case, $\lambda_{hH} \neq 0$ and therefore, we need to introduce two physical states in the following way

$$h_1 = H \cos \alpha + H_{\mu\tau} \sin \alpha, \quad h_2 = -H \sin \alpha + H_{\mu\tau} \cos \alpha,\quad (7)$$

where α is the mixing angle. The above mixing matrix becomes diagonal with respect to the physical states h_1 and h_2 . And the eigenvalues of \mathcal{M}_{scalar}^2 represent the mass terms M_{h_1} and M_{h_2} of the scalar fields h_1 and h_2 respectively. In this work, we choose h_1 as the SM-like Higgs boson. The quartic couplings λ_h , λ_H and λ_{hH} can be expressed in terms of M_{h_1} , M_{h_2} , VEVs (v , $v_{\mu\tau}$) and mixing angle α in the following way

$$\begin{aligned}\lambda_H &= \frac{M_{h_2}^2 + M_{h_1}^2 - (M_{h_1}^2 - M_{h_2}^2) \cos 2\alpha}{4v_{\mu\tau}^2}, \\ \lambda_h &= \frac{M_{h_2}^2 + M_{h_1}^2 - (M_{h_2}^2 - M_{h_1}^2) \cos 2\alpha}{4v_{\mu\tau}^2}, \\ \lambda_{hH} &= -\frac{(M_{h_2}^2 - M_{h_1}^2) \cos \alpha \sin \alpha}{vv_{\mu\tau}}.\end{aligned}\quad (8)$$

Compared to the SM Higgs boson, the couplings of the SM-like Higgs boson h_1 with ordinary particles are suppressed by the factor $\cos \alpha$ in the $U(1)_{L_\mu-L_\tau}$ model, while its couplings to the new gauge boson $Z_{\mu\tau}$ and dark matter ϕ_{DM} are given by

$$\begin{aligned} g_{h_1 Z_{\mu\tau} Z_{\mu\tau}} &= \frac{2M_{Z_{\mu\tau}}^2}{v_{\mu\tau}} \sin \alpha, \\ g_{h_1 \phi_{DM}^\dagger \phi_{DM}} &= -(v\lambda_{Dh} \cos \alpha + v_{\mu\tau}\lambda_{DH} \sin \alpha). \end{aligned} \quad (9)$$

Since $Z_{\mu\tau}$ has a low mass and also it has no couplings to quarks, it can only decay to neutrinos in the framework of $U(1)_{L_\mu-L_\tau}$ model [9]. Without regard to the neutrino masses and mixing, the couplings of $Z_{\mu\tau}$ with neutrinos are as follows

$$g_{Z_{\mu\tau} \nu_\mu \nu_\mu} = \frac{M_{Z_{\mu\tau}}}{v_{\mu\tau}}, \quad g_{Z_{\mu\tau} \nu_\tau \nu_\tau} = -\frac{M_{Z_{\mu\tau}}}{v_{\mu\tau}}. \quad (10)$$

The favored regions of the gauge coupling $g_{\mu\tau}$ and the $Z_{\mu\tau}$ mass to explain the muon $(g-2)$ deviation were summarized in [6]. The regions are

$$2 \times 10^{-4} \leq g_{\mu\tau} \leq 2 \times 10^{-3}, \quad 5 \leq M_{Z_{\mu\tau}} \leq 210 \text{ MeV}. \quad (11)$$

The VEV of ϕ_H is estimated from Eqs. (11) as

$$v_{\mu\tau} = \frac{M_{Z_{\mu\tau}}}{g_{\mu\tau}} \simeq 10 - 1000 \text{ GeV}, \quad (12)$$

which implies that the new ‘‘Higgs’’ boson h_2 emerging with a mass of the same order after the symmetry breaking. It can lead to abundant phenomenology if its mass lies below 125 GeV. The signals of a CP-even scalar boson production with a mass of 100 GeV in the $U(1)_{L_\mu-L_\tau}$ model have been detailedly studied in Ref. [6].

In addition, the scalar mixing is also constrained by analysis of data from the LHC experiments [17] as

$$\sin \alpha \leq 0.3. \quad (13)$$

In our following numerical calculation, the relevant SM input parameters are taken as [18]

$$M_t = 173.07 \text{ GeV}, \quad M_Z = 91.1876 \text{ GeV}, \quad M_{h_1} = 125 \text{ GeV}, \quad \sin^2 \theta_W = 0.231. \quad (14)$$

III. The Light Gauge Boson $Z_{\mu\tau}$ Production at LHC

It can be seen from the previous analysis, $Z_{\mu\tau}$ can not be produced directly due to no couplings to quarks. So we consider the indirect production of $Z_{\mu\tau}$. Besides decaying to SM particles, the SM-like Higgs boson h_1 has extra decay modes to a pair of $Z_{\mu\tau}$ and ϕ_{DM} respectively when $2M_{\phi_{DM}} < M_{h_1}$. We will consider the production of $Z_{\mu\tau}$ via h_1 decaying at LHC. The width expressions of h_1 's two extra decay channels are [9]

$$\Gamma(h_1 \rightarrow Z_{\mu\tau} Z_{\mu\tau}) = \frac{M_{h_1}^3 g_{h_1 Z_{\mu\tau} Z_{\mu\tau}}^2}{128\pi M_{Z_{\mu\tau}}^4} \sqrt{1 - \frac{4M_{Z_{\mu\tau}}^2}{M_{h_1}^2} \left(1 - \frac{4M_{Z_{\mu\tau}}^2}{M_{h_1}^2} + \frac{12M_{Z_{\mu\tau}}^2}{M_{h_1}^4}\right)}, \quad (15)$$

$$\Gamma(h_1 \rightarrow \phi_{DM}^\dagger \phi_{DM}) = \frac{g_{h_1 \phi_{DM}^\dagger \phi_{DM}}^2}{32\pi M_{h_1}} \sqrt{1 - \frac{4M_{DM}^2}{M_{h_1}^2}}, \quad (16)$$

where the M_{DM} is Dark Matter mass. The total decay width of h_1 can be written as

$$\Gamma(h_1) = \cos^2 \alpha \Gamma_{SM} + \Gamma(h_1 \rightarrow Z_{\mu\tau} Z_{\mu\tau}) + \Gamma(h_1 \rightarrow \phi_{DM}^\dagger \phi_{DM}), \quad (17)$$

where Γ_{SM} is the total width of the Higgs boson in SM.

In this model, $Z_{\mu\tau}$ can only decay into neutrinos. Therefore, both of the two extra decay channels are invisible. The branching ratio of the invisible decays in our model is given by

$$BR(h_1 \rightarrow \text{invisibles}) = \frac{\Gamma(h_1 \rightarrow ZZ^*) + \Gamma(h_1 \rightarrow Z_{\mu\tau} Z_{\mu\tau}) + \Gamma(h_1 \rightarrow \phi_{DM}^\dagger \phi_{DM})}{\Gamma(h_1)}, \quad (18)$$

where the $\Gamma(h_1 \rightarrow ZZ^*)$ is the width of decay $h_1 \rightarrow ZZ^* \rightarrow \nu\nu\bar{\nu}\bar{\nu}$ like Higgs in SM. The upper limit on the Higgs boson invisible branching ratio of 0.25 at the 95% CL has been published by the ATLAS Collaboration [19]. With the increase of c.m. energy and integrated luminosity, the collider may give more stringent restrictions in the future.

In a similar situation to SM, there are several production channels of the SM-like Higgs boson, including the associated production with W/Z bosons, the weak vector boson fusion processes, the gluon–gluon fusion processes and the associated production with heavy quarks [20]. The cross sections of different channels for h_1 production in $U(1)_{L_\mu-L_\tau}$ model when we take $\sin\alpha = 0.05$ and $M_{h_1} = 125$ GeV at the 13 TeV LHC are given in Table 3. From the contrast of the cross sections, the gluon–gluon fusion channel can provide the largest event number of h_1 , but this channel $gg \rightarrow h_1 \rightarrow Z_{\mu\tau} Z_{\mu\tau} (Z_{\mu\tau} \rightarrow \nu\bar{\nu}) \rightarrow \cancel{E}_T$ is invisible and hard to be detected in experiment. The second important channel is vector boson fusion, which has a small statistical significance due to the contamination of backgrounds. Higgs associated production with W/Z bosons can provide interesting signals to measure the trilinear coupling, while the signals of associated production with top quarks could measure not only the trilinear coupling but also top-Yukawa coupling, which dominates the renormalization group evolution of the Higgs potential at high energy scales [21–23]. The top-quark Yukawa coupling is among the main drivers of SM predictions at high energies and often dominates in, amongst others, studies of the self-consistency of the SM and in searches for physics beyond the SM [24]. It is of great theoretical and experimental significance to study the signals of the $t\bar{t}h$ production. Thus, we will focus our attention on the signals of $Z_{\mu\tau}$ via $t\bar{t}h$ channel in this work.

Table 3: The cross sections of different channels for h_1 production in $U(1)_{L_\mu-L_\tau}$ model at the 13 TeV LHC.

channels	$\sigma(\text{fb})$
gluon–gluon fusion	14.63
vector boson fusion	3.23
associated production with W/Z bosons	0.39/0.55
associated production with heavy quarks	0.39

Now we consider $Z_{\mu\tau}$ production via h_1 decaying in the $t\bar{t}h_1$ production process at LHC. The relevant Feynman diagrams are shown in Fig. 1. The production of the h_1 with a $t\bar{t}$ pair

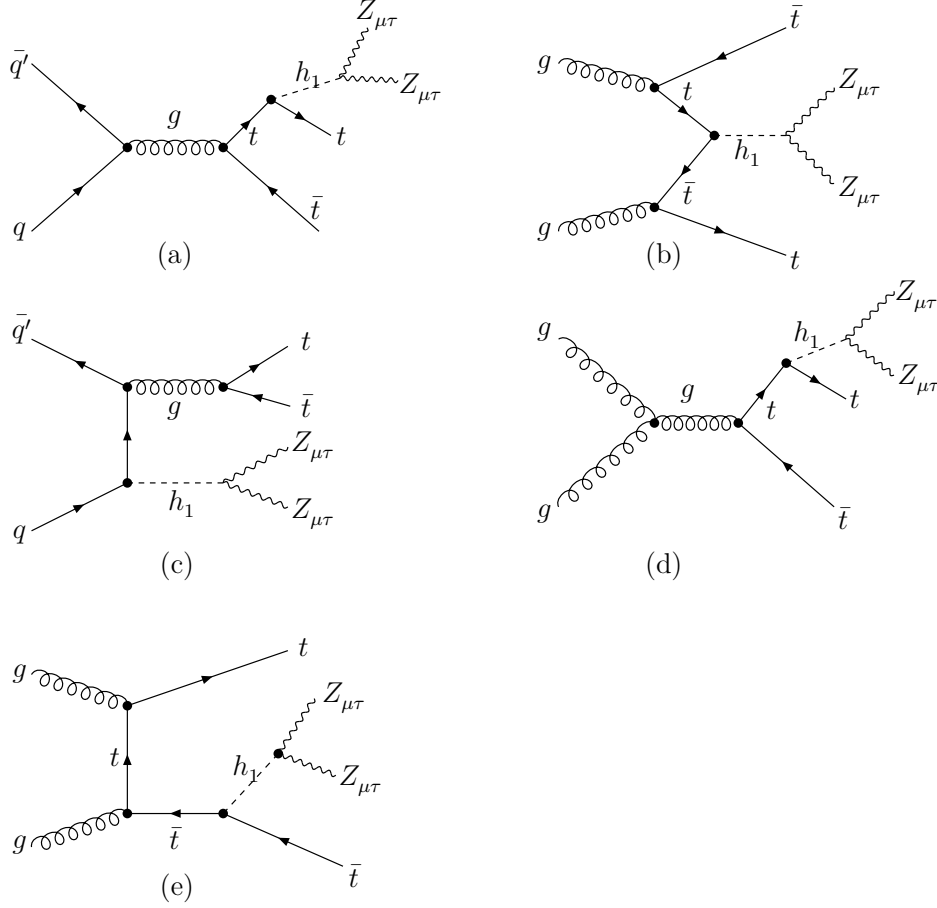


Figure 1: The Feynman diagrams of gauge boson $Z_{\mu\tau}$ production by h_1 decaying in the $t\bar{t}h_1$ production at LHC.

at the LHC is initiated by gluon-gluon interaction at leading order in the perturbation theory. The top-quarks subsequently decay to a b-quark and a boson, while the h_1 can decay in several modes. We choose the channel of h_1 decays to $Z_{\mu\tau}$ as the signals we need. The production cross sections are calculated at tree level by employing Madgraph5/aMC@NLO [25]. Our numerical results are shown in Fig. 2(a) and Fig.2(b), where we plot the $Z_{\mu\tau}$ production cross section as a function of $M_{Z_{\mu\tau}}$ and $\sin\alpha$ respectively for c.m. energy $\sqrt{s} = 13$ TeV (Fig. 2(a) for $\sin\alpha = 0.05$ and Fig. 2(b) for $M_{Z_{\mu\tau}} = 0.1$ GeV). The value of the production cross section σ decreases as $Z_{\mu\tau}$ mass increasing, for $\sin\alpha = 0.05$ and $0.005 \text{ GeV} \leq M_{Z_{\mu\tau}} \leq 0.21 \text{ GeV}$, its value is in the range 0.053 pb to 0.38 pb in Fig. 2(a). From Fig. 2(b), we can see that the values of σ increase abruptly and reach a maximum roughly 0.33 pb for $\sin\alpha = 0.2$. Then, its values vary very little as $\sin\alpha$ increasing. This is because the the production cross section σ is proportional to the factor $\sin^2\alpha(1 - \sin^2\alpha)$.

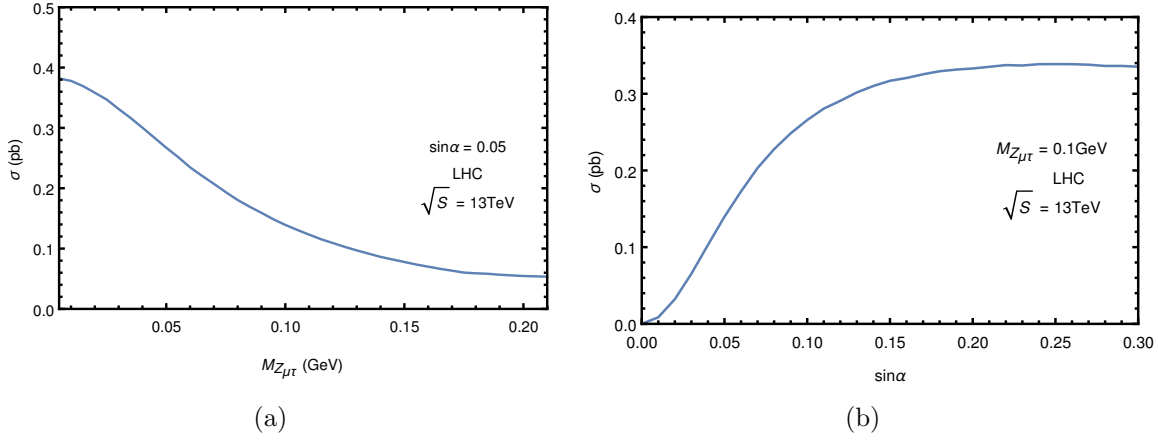


Figure 2: Production cross section as a function of the $Z_{\mu\tau}$ mass (a) and $\sin\alpha$ (b) at the 13 TeV LHC.

IV. Signal and Discovery Potentiality

As we analyzed in Section III, the determination of the associated production of the h_1 with a $t\bar{t}$ pair is of particular importance as the top-quark Yukawa coupling is large and thus an excellent probe for physics beyond SM. In this section, we will use the $pp \rightarrow t\bar{t}h_1(h_1 \rightarrow Z_{\mu\tau}Z_{\mu\tau})$ as a starting point to investigate the observability of $Z_{\mu\tau}$. As mentioned earlier, $Z_{\mu\tau}$ can only decay to neutrinos in this framework. Thus, the signature of $Z_{\mu\tau}$ only is missing energy. The expression of total decay width of $Z_{\mu\tau}$ is given by

$$\Gamma_{Z_{\mu\tau}} = \frac{g_{\mu\tau}^2 M_{Z_{\mu\tau}}}{32\pi}, \quad (19)$$

where we have ignored the neutrino mass and mixing. Then the possible signals of $t\bar{t}Z_{\mu\tau}Z_{\mu\tau}$ for all the decaying channels of the electroweak gauge boson W are

$$\begin{aligned} pp &\rightarrow t(\rightarrow bjj)\bar{t}(\rightarrow \bar{b}jj)h_1(\rightarrow Z_{\mu\tau}Z_{\mu\tau}) \rightarrow b\bar{b}jjjj + \cancel{E}_T \text{ (Hadronic Mode);} \\ pp &\rightarrow t(\rightarrow bl^+\nu_l)\bar{t}(\rightarrow \bar{b}jj)h_1(\rightarrow Z_{\mu\tau}Z_{\mu\tau}) \rightarrow b\bar{b}jjl^+\nu_l + \cancel{E}_T \text{ (Semi-leptonic Mode);} \\ pp &\rightarrow t(\rightarrow bl^+\nu_l)\bar{t}(\rightarrow \bar{b}l^-\bar{\nu}_l)h_1(\rightarrow Z_{\mu\tau}Z_{\mu\tau}) \rightarrow b\bar{b}l^+l^-\bar{\nu}_l\nu_l + \cancel{E}_T \text{ (Purely leptonic Mode);} \\ pp &\rightarrow t(\rightarrow bjj)\bar{t}(\rightarrow \bar{b}l^-\bar{\nu}_l)h_1(\rightarrow Z_{\mu\tau}Z_{\mu\tau}) \rightarrow b\bar{b}jjl^-\bar{\nu}_l + \cancel{E}_T \text{ (Semi-leptonic Mode).} \end{aligned} \quad (20)$$

We focus on the semi-leptonic channel, with one top decaying hadronically and the other decaying leptonically,

$$pp \rightarrow t(\rightarrow bjj)\bar{t}(\rightarrow \bar{b}l^-\bar{\nu}_l)h_1(\rightarrow Z_{\mu\tau}Z_{\mu\tau}) \rightarrow b\bar{b}jjl^-\bar{\nu}_l + \cancel{E}_T \quad (21)$$

where the charged leptons are $l = e, \mu, \tau$. As we can see, the signal contains an isolated charged lepton, two b-jets, two light-quark jets and large missing energy. There are several advantages to studying this channel. First of all, the cross section of the semi-leptonic mode is sizable, about 3 times larger than the cleaner purely leptonic mode. Secondly, one is able to distinguish the t from the \bar{t} using the charge of the lepton in the final state. Thirdly, the SM backgrounds for the hadronic mode are more severe than those for the semi-leptonic mode.

Based on event topology we expect several SM processes to constitute the backgrounds to our signal. The leading SM background is QCD production of top quark pairs, $pp \rightarrow$

$t\bar{t} \rightarrow b\bar{b}jjl^{-}\bar{\nu}_l$ [for $t\bar{t}$]. The cross section for this process is several orders of magnitude larger than our signal. The next background with a large missing energy is $pp \rightarrow t\bar{t}Z(Z \rightarrow \bar{\nu}\nu) \rightarrow b\bar{b}jjl^{-}\bar{\nu}_l\bar{\nu}\nu$ [for $t\bar{t}Z$]. Even though the cross section for this process is smaller than the QCD $t\bar{t}$ by about a factor of 4000, its kinematics are more similar to that of our signal, making such background events difficult to be separated from the signal. Another large SM background is from a process with no top quark, which has a great impact on our signals, $pp \rightarrow W^{-}b\bar{b}jj \rightarrow b\bar{b}jjl^{-}\bar{\nu}_l$ [for $Wb\bar{b}jj$].

Next, we use MadAnalysis5 [26] to present our main results on separating signal events from backgrounds. Although the SM backgrounds have great influences to semi-leptonic decay and $Z_{\mu\tau}$ production, there are many kinematical differences between them that can be exploited. Moreover, we can take full advantage of the observation that the neutrino from W decay is largely responsible for the \cancel{E}_T in the $t\bar{t}$ and $Wb\bar{b}jj$ backgrounds, while it contributes only a fraction of \cancel{E}_T in the signal.

For the following results we use the FeynRules [27] to implement the UFO [28] format of the $U(1)_{L_{\mu}-L_{\tau}}$ model, Madgraph5/aMC@NLO [25] to generate signal and background events, PYTHIA [29] for parton shower and hadronization and DELPHES [30] as fast detector simulation with ATLAS detector card. Finally, MadAnalysis5 [31] is applied for data analysis and plotting.

We can use some cuts of kinematic distributions to reduce the background contribution and enhance the signal. We show the normalized distributions of the total miss transverse energy \cancel{E}_T , the missing transverse hadronic energy \cancel{H}_T and the transverse mass $M_T[l]$ in the Fig. 3. From the Fig. 3 (a), (b) and (c), we see that a missing transverse hadronic energy $\cancel{H}_T > 110$ GeV, a large missing energy cut of $\cancel{E}_T > 115$ GeV and the transverse mass $M_T[l] > 100$ GeV could be imposed to effectively remove the $Wb\bar{b}jj$ and $t\bar{t}$ backgrounds. But, the $t\bar{t}Z$ is difficult to be separated from the signal all the way. There are in principle other variables which we could use to distinguish signal from background. However, these variables are largely similar, and unlikely to do significantly better than the \cancel{H}_T , \cancel{E}_T and $M_T[l]$ variables presented here. According to the above analysis, events are selected to satisfy the following cuts:

$$\begin{aligned}
\text{Cut - 1} & : M_{HT} > 110 \text{ GeV}; \\
\text{Cut - 2} & : MET > 115 \text{ GeV}; \\
\text{Cut - 3} & : M_T(l) > 100 \text{ GeV}.
\end{aligned}
\tag{22}$$

After all kinematical cuts are applied, the event numbers of signal and the backgrounds are summarized in Table 4. We defined the statistical significance as $S/\sqrt{S+B}$ where S and B denote the number of signal and background events, respectively [32]. The significance of 2.0 can be obtained when we take $\sin\alpha = 0.05$, $M_{Z_{\mu\tau}} = 0.1$ GeV and integrated luminosity of 300 fb^{-1} .

The integrated luminosities necessary for observing the light gauge boson $Z_{\mu\tau}$ at the 3σ and 5σ levels at the 13 TeV LHC with different $\sin\alpha$ are plotted as a function of $M_{Z_{\mu\tau}}$ in Fig. 4. From Fig. 4, we see that we can obtain larger significance for larger $\sin\alpha$ and smaller $M_{Z_{\mu\tau}}$ within their limits. Therefore, we can find the signal of $Z_{\mu\tau}$ at 13 TeV LHC or future colliders with sufficient integrated luminosities and proper values of $\sin\alpha$ and $M_{Z_{\mu\tau}}$ theoretically in this model.

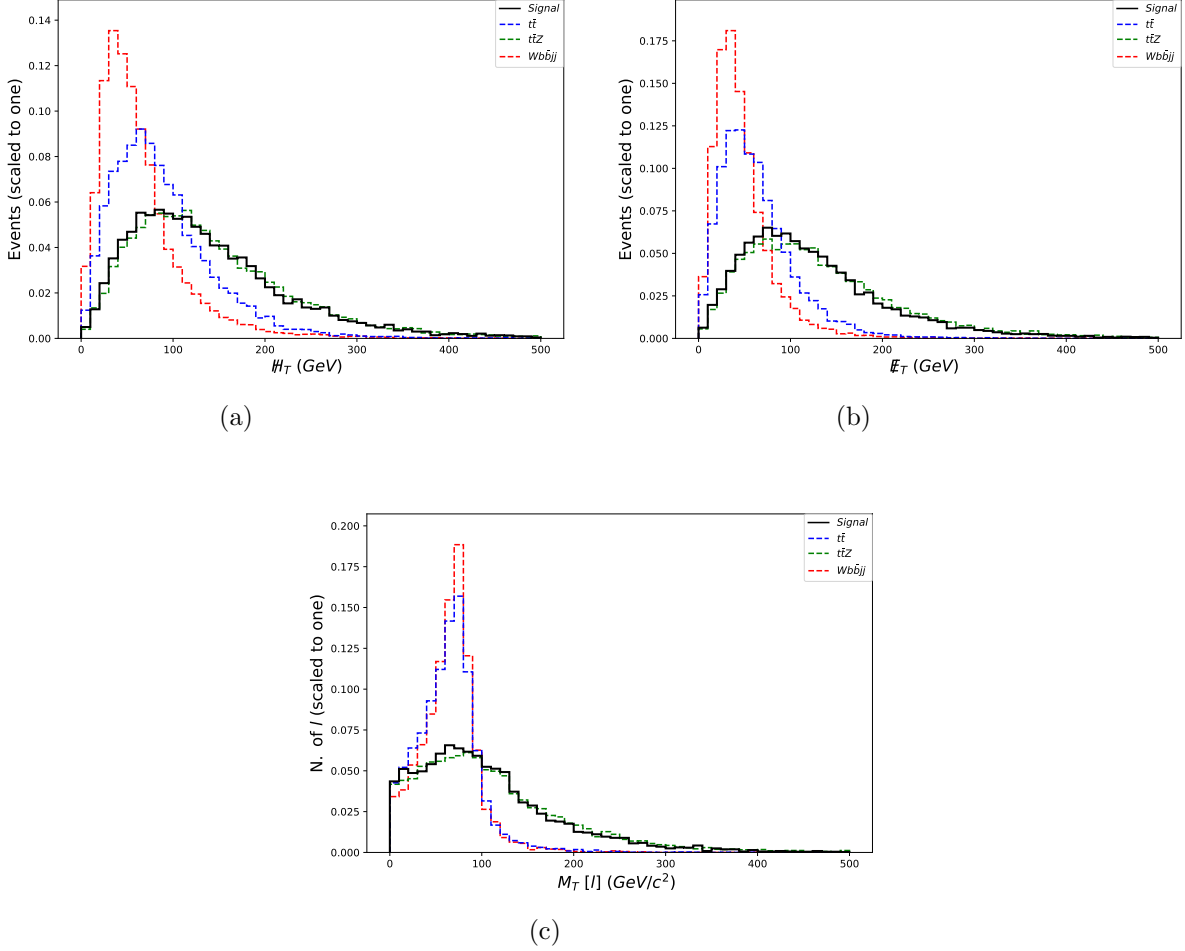


Figure 3: Normalized distributions of \mathcal{H}_T (a), \mathcal{E}_T (b) and $M_T[l]$ (c) for the signal at the LHC with the $\sqrt{s} = 13$ TeV and an integrated luminosity of 300 fb^{-1} .

Table 4: Effect of individual kinematical cuts on the signal for $M_{Z_{\mu\tau}} = 0.1$ GeV and $\sin\alpha = 0.05$ and background. The statistical significance is computed for a luminosity of 300 fb^{-1} .

Cuts	Signal(S)	Background(B)	$S/\sqrt{S+B}$
Initial(no cut)	4712	2.9×10^7	0.881
Cut 1	2633	6.6×10^6	1.03
Cut 2	1970	2.24×10^6	1.31
Cut 3	633	9.9×10^4	2.0

IV. Conclusions

In this paper, we discuss the possibility of searching for the new gauge boson $Z_{\mu\tau}$ predicted by the $U(1)_{L_{\mu}-L_{\tau}}$ model via $t\bar{t}h_1$ production at LHC. We first calculate the production cross section of the process $pp \rightarrow t\bar{t}Z_{\mu\tau}Z_{\mu\tau}$ in reasonable parameter space of this model. Then, we investigate the observability of the $Z_{\mu\tau}$ boson production through the $pp \rightarrow t(\rightarrow bjj)\bar{t}(\rightarrow \bar{b}l^{-}\bar{\nu}_l)h_1(\rightarrow Z_{\mu\tau}Z_{\mu\tau}) \rightarrow b\bar{b}jjl^{-}\bar{\nu}_l + \cancel{E}_T$ process. After simulating the signal as well as the relevant backgrounds, and applying suitable kinematic cuts, the statistical significance can

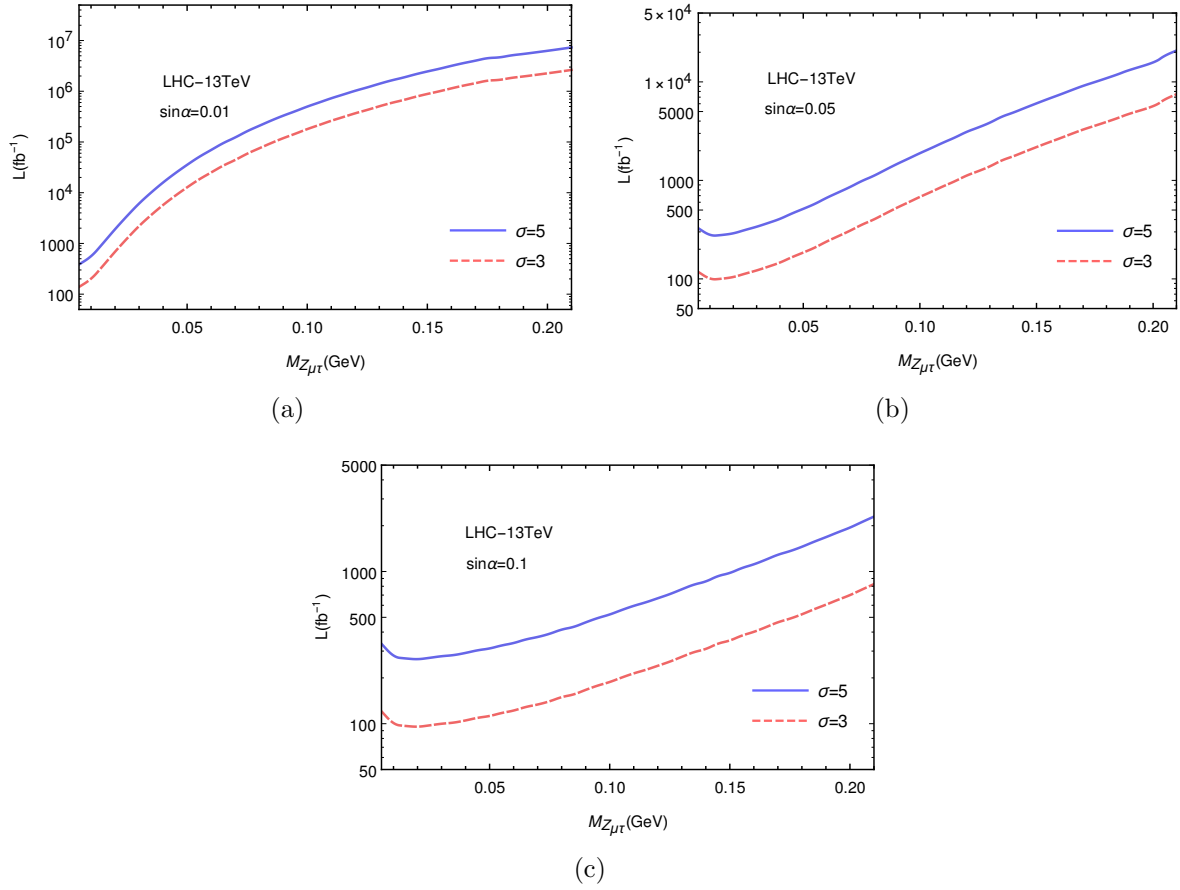


Figure 4: The needed luminosity to observe different masses of $Z_{\mu\tau}$ for 3σ and 5σ statistical significances with different scalar mixing $\sin\alpha$ at the 13 TeV LHC.

reach 2.0 when we take $\sin\alpha = 0.05$ and $M_{Z_{\mu\tau}} = 0.1$ GeV at the 13 TeV LHC with an integrated luminosity of 300 fb^{-1} . Thus, with sufficient integrated luminosity and proper value of $\sin\alpha$ and $M_{Z_{\mu\tau}}$, the signal of $Z_{\mu\tau}$ might be detected at the 13 TeV LHC or future colliders.

ACKNOWLEDGEMENT

One of us (J.X.H.) would thank Zhen-hua Zhao for reading the manuscript. This work was supported in part by the National Natural Science Foundation of China under Grant No. 11275088 and Grants No. 11747318.

References

- [1] Q. R. Ahmad et al. [SNO Collaboration], Phys. Rev. Lett. 89, 011301 (2002).
- [2] G. W. Bennett et al. [Muon g-2 Collaboration], Phys. Rev. D 73, 072003 (2006) [hep-ex/0602035].
- [3] C. Patrignani et al. [Particle Data Group], Chin. Phys. C 40, no. 10, 100001 (2016).

- [4] F. Jegerlehner and R. Szafron, Eur. Phys. J. C 71, 1632 (2011).
- [5] K. Hagiwara, R. Liao, A. D. Martin, D. Nomura and T. Teubner, J. Phys. G 38, 085003 (2011).
- [6] T. Nomura and T. Shimomura, “Light Z' boson from scalar boson decay at collider experiments in an $U(1)_{L_\mu-L_\tau}$ model”, arXiv:1803.00842 [hep-ph].
- [7] A. Biswas, S. Choubey and S. Khan, “Neutrino Mass, Dark Matter and Anomalous Magnetic Moment of Muon in a $U(1)_{L_\mu-L_\tau}$ Model” JHEP 1609, 147 (2016).
- [8] W. Altmannshofer, S. Gori, S. Profumo and F. S. Queiroz, “Explaining Dark Matter and B Decay Anomalies with an $L_\mu - L_\tau$ Model” JHEP12(2016)106, arXiv:1609.04026 [hep-ph].
- [9] A. Biswas, S. Choubey, and S. Khan, “FIMP and Muon $(g - 2)$ in a $U(1)_{L_\mu-L_\tau}$ Model” JHEP02(2017)123, arXiv:1612.03067 [hep-ph].
- [10] M. G. Aartsen et al. [IceCube Collaboration], Phys. Rev. Lett. 113, 101101 (2014) [arXiv:1405.5303 [astro-ph.HE]].
- [11] A. Kamada and H. B. Yu, Phys. Rev. D 92, no. 11, 113004 (2015) [arXiv:1504.00711 [hep-ph]].
- [12] A. DiFranzo and D. Hooper, Phys. Rev. D 92, no. 9, 095007 (2015) [arXiv:1507.03015 [hep-ph]].
- [13] T. Araki, F. Kaneko, T. Ota, J. Sato and T. Shimomura, Phys. Rev. D 93, no. 1, 013014 (2016) [arXiv:1508.07471 [hep-ph]].
- [14] D. Banerjee et al. [NA64 Collaboration], arXiv:1710.00971 [hep-ex].
- [15] M. Anelli et al. [SHiP Collaboration], arXiv:1504.04956 [physics.ins-det].
- [16] T. Abe et al. [Belle-II Collaboration], arXiv:1011.0352 [physics.ins-det].
- [17] K. Cheung, P. Ko, J. S. Lee and P. Y. Tseng, JHEP 1510, 057 (2015).
- [18] M. Tanabashi et al. (Particle Data Group), Phys. Rev. D 98, 030001 (2018).
- [19] G. Aad et al. [ATLAS Collaboration], JHEP 1511 (2015) 206 [arXiv:1509.00672 [hep-ex]].
- [20] A. Djouad et al. “The Anatomy of electro-weak symmetry breaking. I: The Higgs boson in the standard model”, Phys.Rept. 457 (2008) 1-216 [hep-ph/0503172].
- [21] G. Degrandi, S. Di Vita, J. Elias-Miro, J. R. Espinosa, G. F. Giudice, G. Isidori and A. Strumia, JHEP 1208, 098 (2012) [arXiv:1205.6497 [hep-ph]].
- [22] S. Alekhin, A. Djouadi and S. Moch, Phys. Lett. B 716, 214 (2012) [arXiv:1207.0980 [hep-ph]].

- [23] D. Buttazzo, G. Degrassi, P. P. Giardino, G. F. Giudice, F. Sala, A. Salvio and A. Strumia, JHEP 1312, 089 (2013) [arXiv:1307.3536 [hep-ph]].
- [24] S. Boselli, R. Hunter, A. Mitov, “Prospects for the determination of the top-quark Yukawa coupling at future e^+e^- colliders”, arXiv:1805.12027 [hep-ph].
- [25] J. Alwall et al., JHEP 07, 079 (2014).
- [26] E. Conte, B. Fuks, and G. Serret, Comput.Phys.Commun. 184 (2013) 222-256.
- [27] A. Alloul, N. D. Christensen, C. Degrande, C. Duhr, and B. Fuks, Comput. Phys. Commun. 185 (2014) 22502300.
- [28] N. D. Christensen and C. Duhr, Comput. Phys. Commun. 180, 1614-1641 (2009).
- [29] T. Sjostrand, S. Mrenna and P. Z. Skands, JHEP 0605 (2006) 026.
- [30] DELPHES 3 Collaboration, JHEP 1402 (2014) 057.
- [31] E. Conte, B. Fuks and G. Serret, Comput. Phys. Commun. 184, (2013) 222.
- [32] Hai Y W and Bing F Y, “Top partner production at e^+e^- collider in the littlest Higgs Model with T-parity”, arXiv:1706.02821 [hep-ph].